Hydrocarbon Reservoir Potential of the Mississippian Chainman Shale, Western Utah

Bereskin & Associates

S. Robert Bereskin, Bereskin and Associates

Thomas C. Chidsey, Jr., Utah Geological Survey

The University of Utah

John D. McLennan, University of Utah

Craig D. Morgan, Utah Geological Survey

Abstract

Examination and sampling of a ~500-m surface section of the Mississippian Chainman Shale from the Confusion Range of western Utah indicates that it possesses clear potential for hydrocarbon production. Although very good stratigraphic and geochemical work has been published, this evaluation of the Chainman revealed previously unrecognized reservoir potential, particularly in the lower 300 m of the formation. Although total organic carbon measurements are uniformly modest (1-2 wt%), new laboratory analysis reveals adequate mudrock porosity (3 to 9% effective) and oil saturation for largely liquid hydrocarbon production. In fact, one surface sample surprisingly contained substantial amounts of mobile oil (8%). Of the four major unconventional reservoir types recognized (organic siltstone, argillaceous mudstone, calcareous mudstone, and siliceous mudstone), the siliceous mudstone and organic siltstone most likely represent the "sweet spot" lithologies in the Chainman of western Utah. If some gross subsurface assumptions are made, including a normally pressured well at 1600-m drilling depth, a 20% water saturation, a 20% recovery factor, estimations of recoverable oil on an 80-acre spacing would amount to 270,000 BO and 1.5 BCFG over a 20-year lifespan. This estimate is based on surface mapping and geochemical testing exclusively.

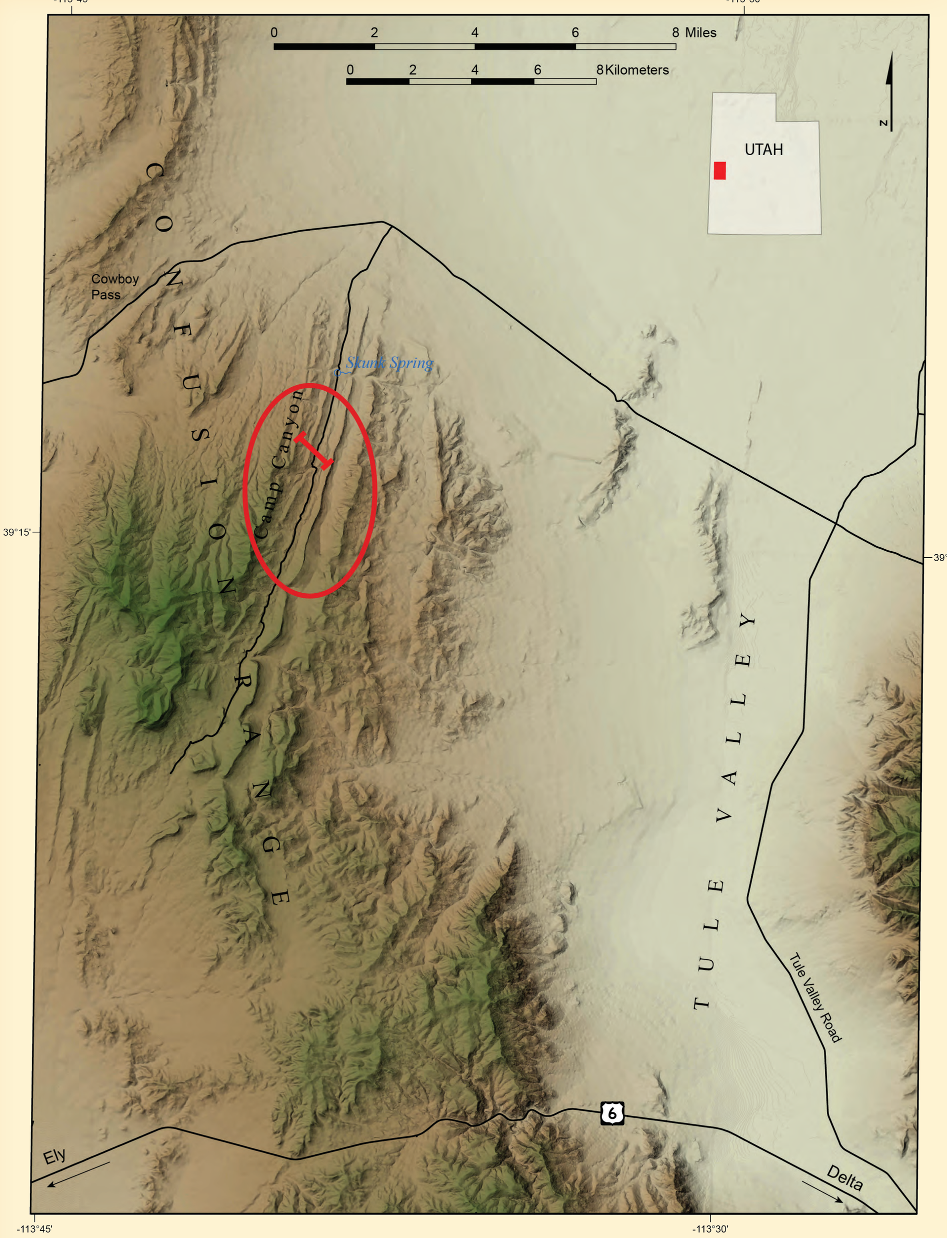

Location map of the Camp Canyon study site and measured section for the Chainman Shale, central Confusion Range, western Utah.

Stratigraphic Column of the Chainman Shale, Confusion Range

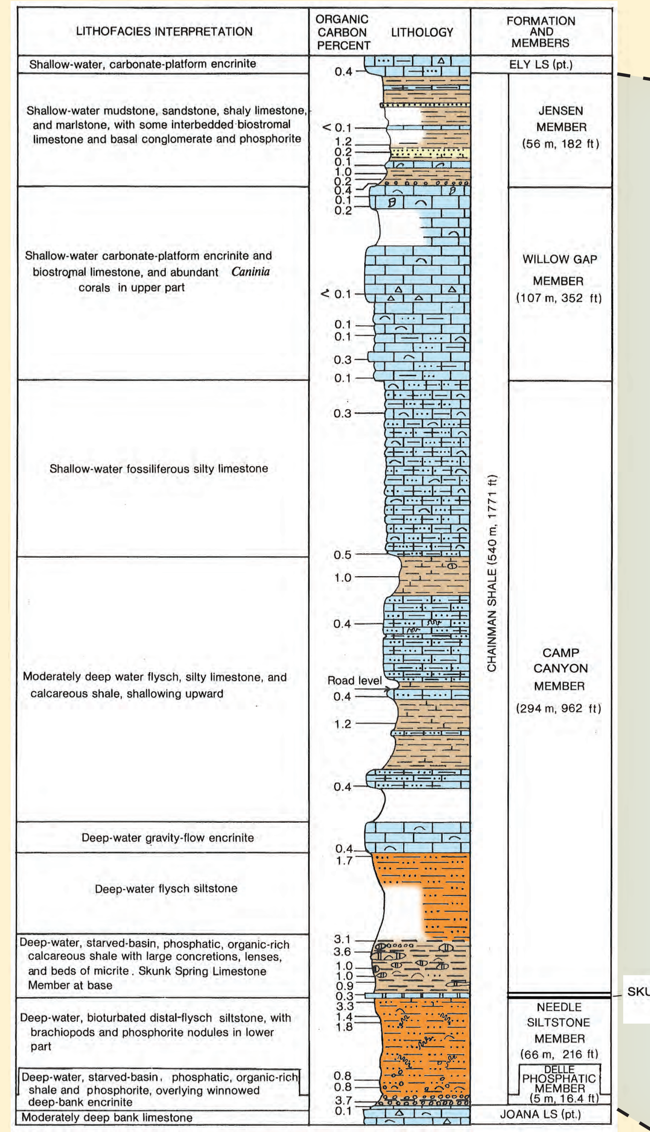

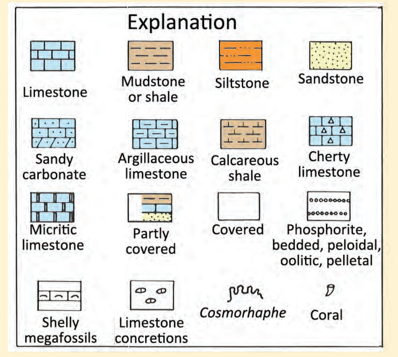

Modified from Sadlick (1965); Sandberg and others (1980); Hintze and Davis (2003).

Gamma-Ray Log of the Chainman Shale, Camp Canyon Section.

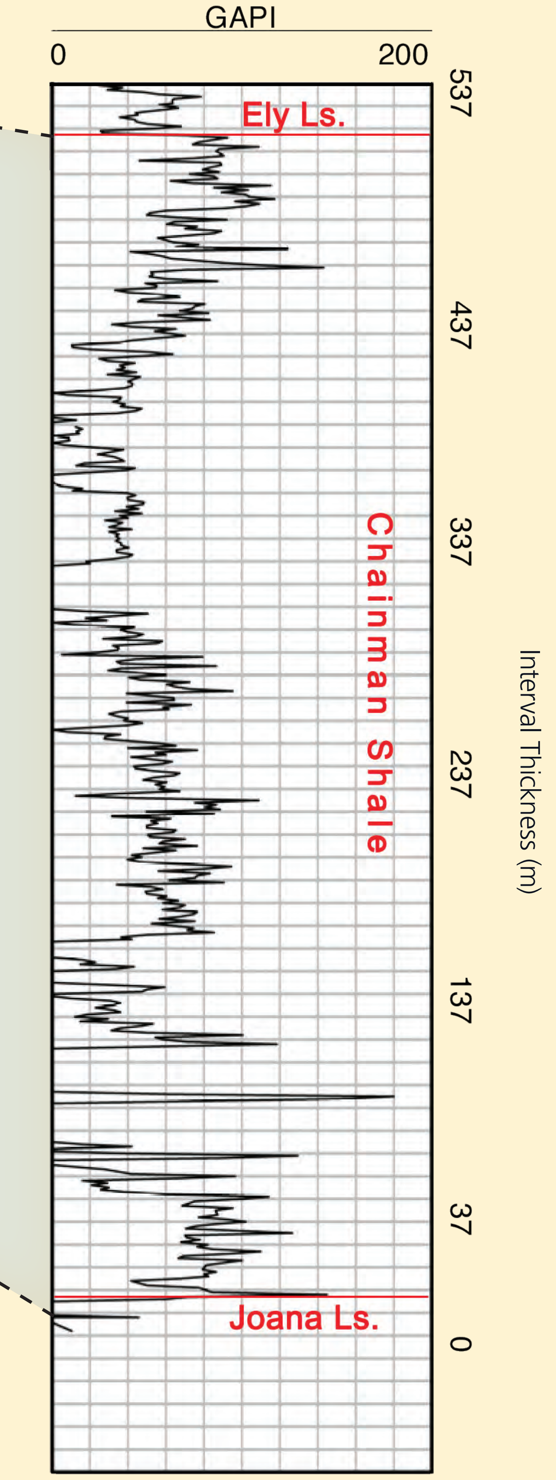

The preferential occurrence of organic carbon is shown in the lower part of the Chainman Shale (Skunk Spring Limestone, Needle Siltstone, Phosphatic Members).

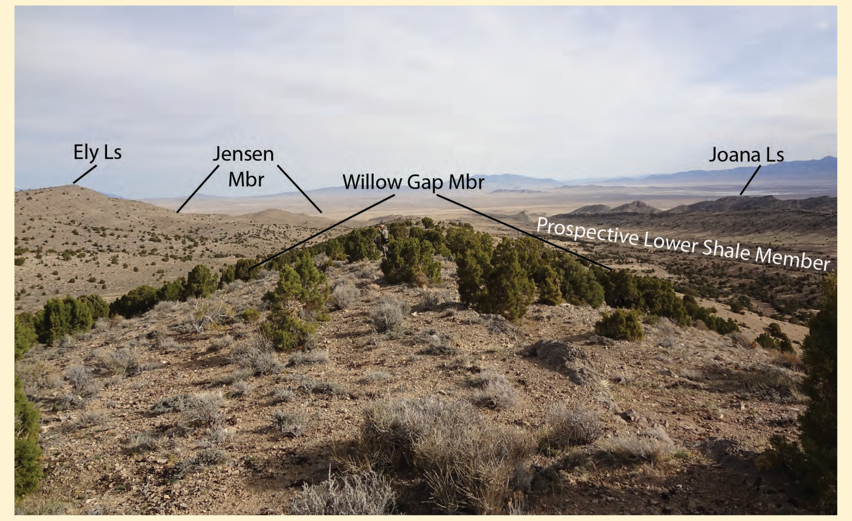

Typical outcrop of the Chainman Shale, Camp Canyon, Confusion Range.

View north along the topographically resistant Willow Gap Member, the unit that markedly contrasts with the two recessive Chainman units above (left) and stratigraphically below (right). On the right, one can readily see the locally resistant organic limestone ridges or "ribs," characteristic within the mudrock-rich section. The boldly resistant ridge on the right is reflective of the underlying Joana Limestone. The recessive unit to the left is the Jensen Member and to the right is the Camp Canyon Member. The Chainman Shale is overlain by the Ely Limestone (resistant material on left just beneath the skyline).

Measured Section of the Chainman Shale, Camp Canyon, Confusion Range

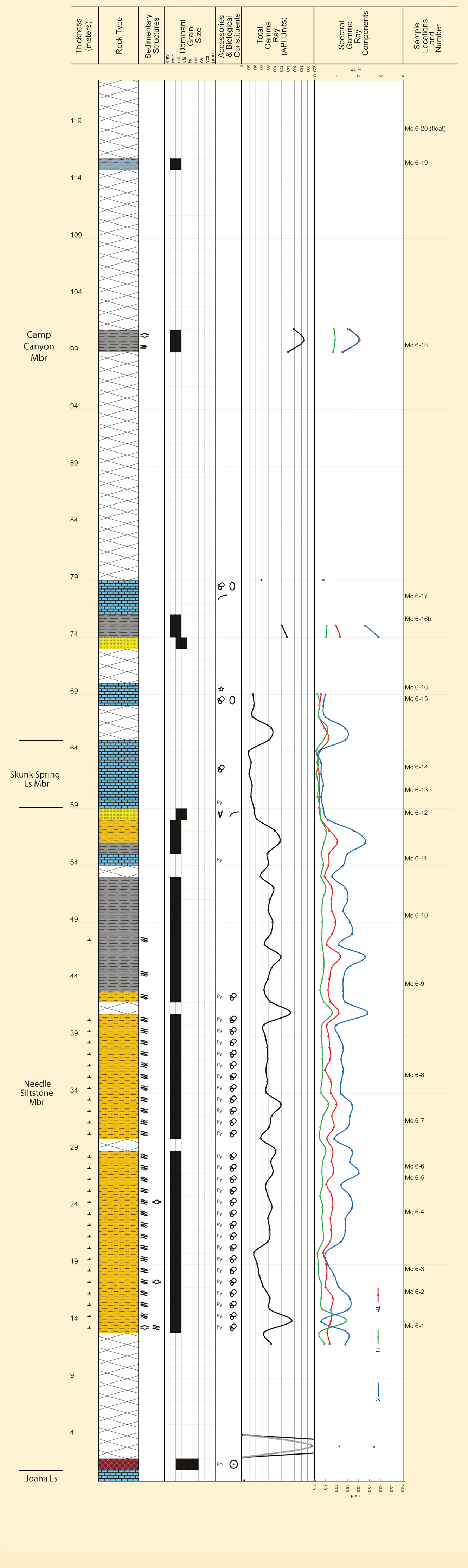

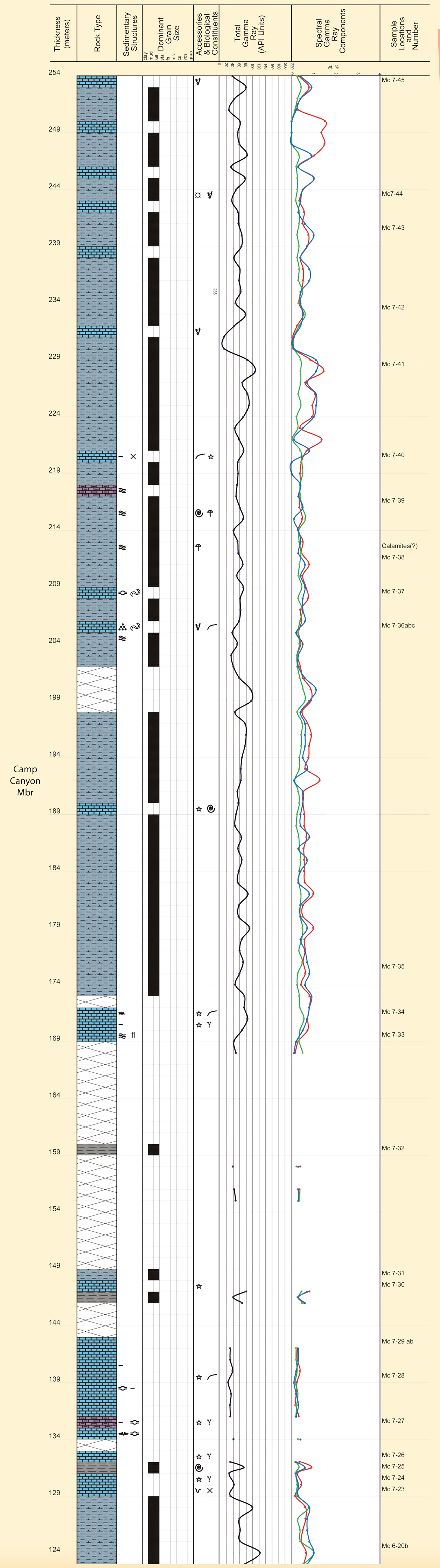

Most Chainman Shale facies likely reflect offshore marine, both quiet water and current-swept deposition at higher stratigraphic levels. Strata contained in the stratigraphic column from the base to 254 m belong to four distinguishable lithostratigraphic intervals:

1. The lowest interval (lithostratigraphic interval 1) resting on the Joana Limestone is a dark gray layered phosphate (Delle Phosphatic Member); however, much of this lower material is not exposed.
2. A dark gray, poorly sorted, muddy siltstone (lithostratigraphic interval 2) forms the lower part of the Needle Siltstone Member.
3. Interbedded dark gray to black, organic, calcareous to noncalcareous mudstone comprises most of the potential "shale" pay (lithostratigraphic interval 3), the Skunk Spring Limestone and lower Camp Canyon Members.
4. Interbedded fine-grained, muddy, organic limestones of the Camp Canyon Member form the fourth group (lithostratigraphic interval 4).

The very dark gray to dark green-gray phosphatic beds representing lithostratigraphic interval 1 occur in the form of dominant lumps, ooids, and cement(?), admixed with lesser amounts of silt and sand-sized terrigenous clastics and rare fossils (conodonts, arenaceous forams). Some of the greenish samples may have been partly glauconitic; such glauconite-phosphate assemblages commonly occur at the bases of transgressive systems tracts (TST) (e.g., basal Delle Phosphatic Member overlying the Joana Limestone).

An orange-brown weathering, recessive siltstone overlies the phosphatic interval 1 (lithostratigraphic interval 2). The fresh surface is dark gray due to modest amounts of organic content (see 0.94% TOC measurement for Mc 6-2). The poorly sorted, coarse silt/very fine grained sand is mainly composed of quartz and feldspar admixed with some mud (clay) and appreciable diagenetic dolomite, organics, pyrite, common muscovite, rare glauconite, some bioturbation, and arenaceous forams.

The Chainman shales (lithostratigraphic interval 3) are dark gray to dark brown-gray on fresh surfaces, but weather to a pale orange-gray in many instances. Most mudrocks are calcareous to some degree although a subordinate portion is noncalcareous and decidedly clay-rich. Organic content is variable, but TOC values should be regarded as minimal because of potential loss during surface or near-surface weathering. Other shale ingredients (besides calcite and clay) include terrigenous silt, some dolomite, and omnipresent pyrite. Biotics are variable and include sponge spicules, Foraminifera, nautiloids, goniatites, inarticulate brachiopods, plant material, and numerous trace fossils (some bioturbation is locally abundant and intricate).

The limestone units often occur as isolated interbeds (lithostratigraphic interval 4), but can form very resistant ridges when appreciably thick. Many limestone units appear very dark (organic), especially very low and very high stratigraphically, and apparently formed in quiet-water offshore settings. Other limestone units (sometimes containing distinct nodules), belonging to the "middle" portion of the lower 254-m interval are diversely bioclastic and probably resulted from downslope movement and accumulation. Common megafossils include pelmatozoans, brachiopods, cephalopods, and bryozoans. Some of these reworked carbonates exhibit ripples, cross-bedding, common rip-ups, mud flasers, and distinct flute and/or groove casts.

Explanation

- Limestone Conglomerate
- Limestone
- Covered Interval
- Muddy Limestone
- Packstone
- Sandstone
- Sandy Limestone
- Shale or Mudstone - Calcareous
- Shale or Mudstone - Poorly Calcareous
- Siliceous or Layered Phosphate
- Siltstone
- Silty Limestone

- Bioturbated
- Bryozoan
- Calcitic
- Carbonaceous
- Cephalopod
- Cross-Lamination or Bedding
- Erosion Surface
- Flaser Bedding
- Gastropod
- Grading
- Loading
- Microfossil
- Mottled
- Muddy Remnant
- Nodular

- Oolitic
- Ostracod
- Pelmatozoan
- Peloid
- Ph Phosphatic
- Planar Lamination
- Py Pyritic
- Rip-Up or Breccia Clast
- Rippled
- Rugose Coral
- Shell Fragment
- Soft-Sediment Deformation
- Sponge Spicule
- Stylolitic
- Trilobite
- Wavy Lamination

Apart from the recessive, organic, dark gray calcareous or noncalcareous shales or mudrocks, from 260 to 266 m, the remainder of the column (266 m to the top of the section) can be separated into two major lithostratigraphic intervals that differ from lithostratigraphic intervals 1 through 4 in the lower half of the section:

5. Very thick and resistant, light brown-gray to medium dark gray, muddy to distinctly bioclastic limestones of the upper Camp Canyon and Willow Gap Members.
6. Recessive beds of orange-brown weathered silty/sandy limestones, calcareous sandstones/siltstones, and minor amounts of recognizable shales or claystones constitute the Jensen Member.

Separating these two major intervals is a phosphate (at 458-459 m), similar to that recognized at the base of the Chainman (lithostratigraphic interval 1). This phosphate may rest on a subtle and somewhat debatable karstified limestone, where a reddening of the limestone and accompanying red-stained veins may point to some dissolution in a near-subaerial setting. The phosphate itself represents the base of another TST, and again contains lumps, ooids, and cement in association with calcitic fossil fragments, calcite cement, and some obvious mesopores. As the phosphate disappears upward, a light to medium gray, thin limestone conglomerate prevails, representing erosion and redeposition of offshore marine carbonates as well as reworking of ramose bryozoans. Above that bed, the uppermost orange-brown mixed rocks (lithostratigraphic interval 6) become more evident along with covered slopes of probable green-hued claystone and some dark gray organic mud (sample no. 486).

With respect to the limestone interval (lithostratigraphic interval 5), the lower portion (255 to 352 m) is largely micritic mudstones and wackestones, and commonly wavy bedded and associated with dark gray shale partings/interbeds, bioturbation, and additional thin interbeds of lighter-hued claystone. Above 352 m, light brown-gray bioclastic limestones appear (largely packstones and grainstones), likely reflecting shallowing conditions. Many sedimentary structures include trough and low-angle planar cross-bedding, localized grading, and rip-ups. Fining upward trends occur within stratigraphically restricted packages. The bioclastic limestones can be very coarse grained, and more shallow-water faunal elements include omnipresent pelmatozoans, thick-shelled productid and spiriferid brachiopods (some in clearly a transported position; convex upward disarticulated shells at 375.5 m), e.g.,solitary and compound rugose corals, bryozoans, and instances of vertical trace fossils akin to *Skolithus* (at 396 m). Scattered goniatites and nautiloids may indicate open-ocean conditions, and oncoids (at 378 m) perhaps reflect the shallow subtidal conditions that may be a fitting depositional setting for the overall bioclastic assemblage.

Above the limestone beds and intervening phosphate, the orange-brown weathered exposures (lithostratigraphic interval 6) mainly represent a series of mixed rocks in which terrigenous clastics and carbonate material were subjected to some apparently gentle current activity. Current ripples, cross-lamination, and wavy lamination are common, but so are bioturbation and numerous megafossils, including bryozoans, pelmatozoans, brachiopods, and (more rare) trilobites and echinoderms. These shallow-marine deposits may reflect tidal-flat settings with periodic exposure accounting for the comparatively high iron content (now "limonitic").

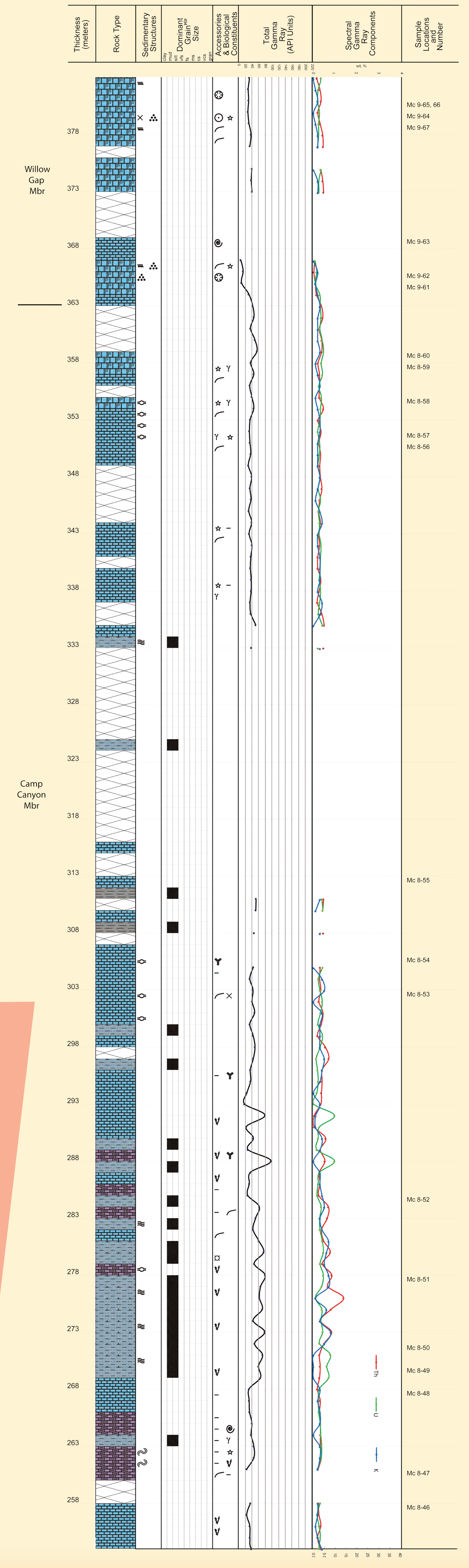

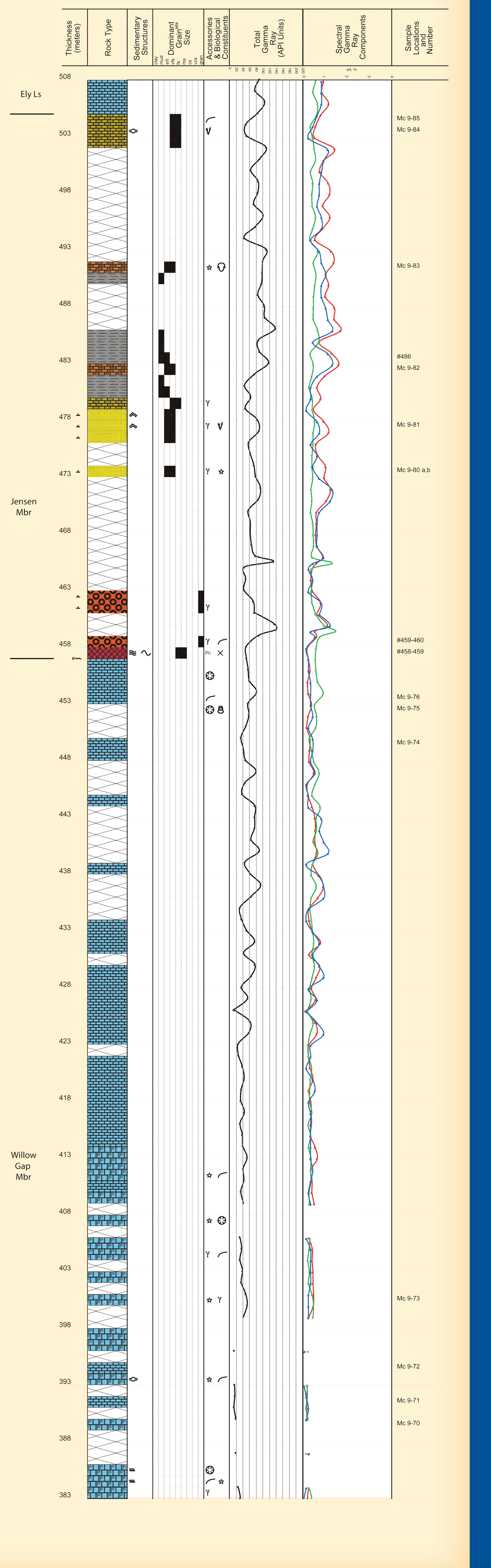

Petrography

Basal Beds

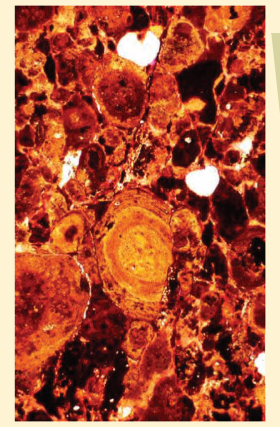

Base of formation is represented by a dense phosphate accumulation common to lower portions of a transgressive systems tract. Phosphate is in the form of lumps, ooids, and cements--all admixed with a small percentage of terrigenous clastics (white grains). Very dark material is likely a combination of organic material and replacive pyrite. Plane polarized light (40x)

Sample— MC 6-2

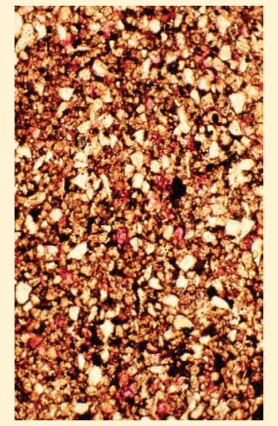

High magnification view of the dolomitic siltstone demonstrates the poor sorting of the white terrigenous material as well as its pronounced angularity. Most of the brownish material is authigenic dolomite. The black material is reflective of pyrite/organics, and the magenta hues indicate the presence of some porosity (approximating 3%). Plane polarized light (100x)

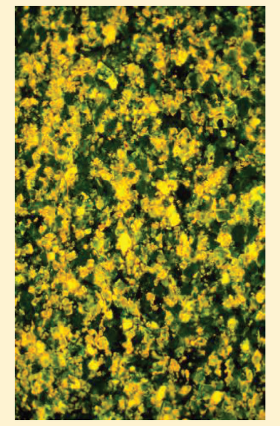

Reflected light example of the image to the left demonstrates opacity of grains in the green to black hues, mineral fluorescence from the dolomite appears as yellow, and for the most part, void space is qualitatively revealed in subtle shades of orange. Reflected ultra-violet light with blue-violet filter (100x)

Sample— MC 6-9

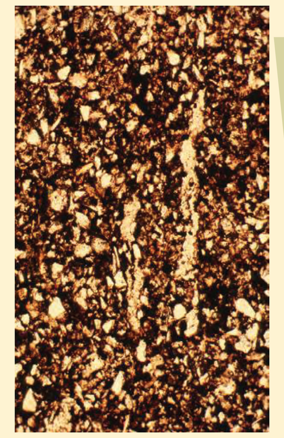

This sample shows two crushed and compacted arenaceous forams in a silty, muddy matrix. Although this silty interval is not really a mudrock, such clastically diluted muds(?) may be important from a potential hydrocarbon perspective because of the facies appreciable thickness (see measured section on Panel I). Plane polarized light (100x)

Sample— MC 6-16B

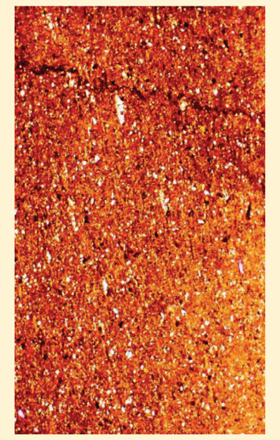

This sample is representative of a very thick (40 m), dark gray, noncalcareous mudrock, rich in clay and modestly silty (see measured section, Panel I). White grains in this view represent the fairly common presence of arenaceous forams. Organic content is also significant, at least 1.63%, and the porosity is comparatively high for siltstones, due perhaps to the presence of leached fossils here and to the probable weathered state of the sample. Plane polarized light (40x)

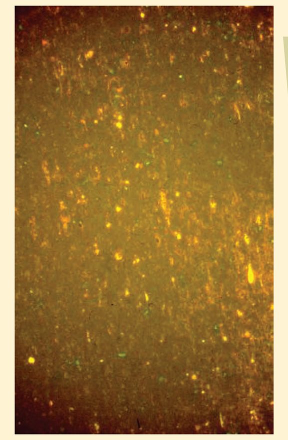

Porosity-only image of the image to the left indicates two void types in this noncalcareous mudrock. The yellow color is indicative of leached microfossils, and the orange hues represent smaller and tighter micropores from the dominant clay matrix. Green, again, is opaque material. Reflected ultra-violet light with blue-violet filter (40x)

Sample— MC 9-86

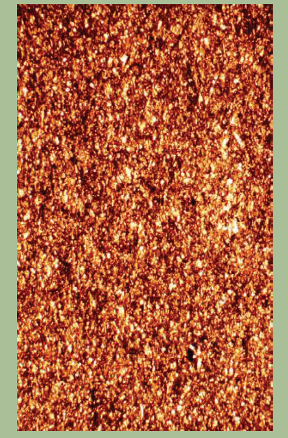

This specimen represents a "grab" sample taken at approximately 185 m from the base of the formation. This calcareous mudstone is consistent with other examples of the sandy limestone facies. In spite of the abundance of silica and other insoluble framework grains, a TOC of 1.26% was obtained here. The Tmax clearly indicates a source bed in the oil-generating window. Whereas most TOC numbers are quite modest in this surface study, these values are important enough when considering the total thickness of the potential shale package as specifically measured in this western Utah setting. Plane polarized light (40x)

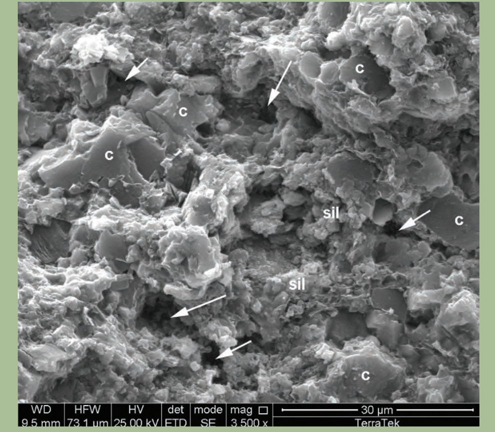

SEM image of silt-sized calcic fossil fragments (c) and the porous siliceous matrix (sil). The largest pores are 5-10 microns across (arrows), and appear to be well-connected in a permeable network of matrix micropores. Scale bar = 30 microns

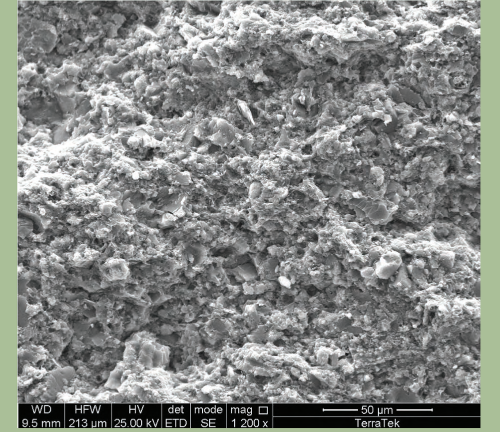

High magnification SEM image showing the granular microtexture that is characteristic of a siliceous matrix. Scale bar = 50 microns

Petrophysical Properties

Tight rock analysis data of Chainman Shale from the Camp Canyon section (see measured section for sample locations in meters).

Sample ID	As Received Bulk Density (g/cc)	As Received Grain Density (g/cc)	Effective Dry Grain Density (g/cc)	Effective Porosity (% of BV*)	Water Saturation (% of PV†)	Gas Saturation (% of PV)	Mobile Oil Saturation (% of PV)	Gas-Filled Porosity (% of BV)	Bound Hydrocarbon Saturation (% of BV)	Bound Clay Water (% of BV)	Pressure-Decay Permeability (nD)
Sample 486	2.325	2.349	2.542	13.42	91.71	7.72	0.58	1.04	0.08	21.02	177
Mc-8-49	2.399	2.615	2.637	9.48	11.71	87.45	0.84	8.29	0.01	7.90	51
Mc-9-86	2.504	2.604	2.627	5.14	23.59	74.79	1.62	3.84	0.15	4.35	106
Mc-6-16b	2.409	2.558	2.573	6.74	11.90	86.91	1.19	5.85	0.01	9.09	112
Mc-6-6	2.633	2.710	2.716	3.16	2.47	89.81	7.72	2.83	0.10	2.48	173
Mc-6-2	2.593	2.676	2.682	3.46	8.29	90.32	1.38	3.13	0.01	4.02	78

* BV – bulk volume
† PV – pore volume

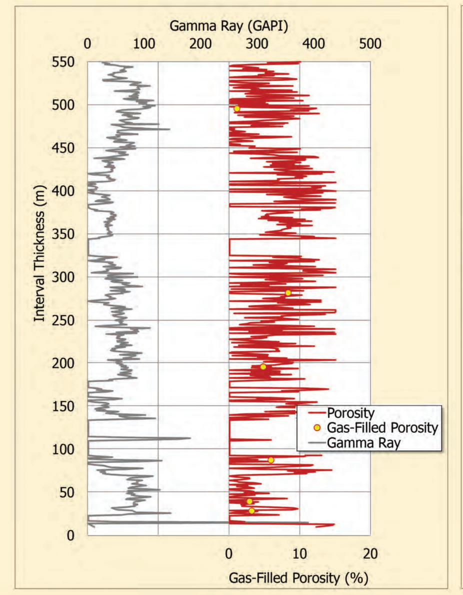

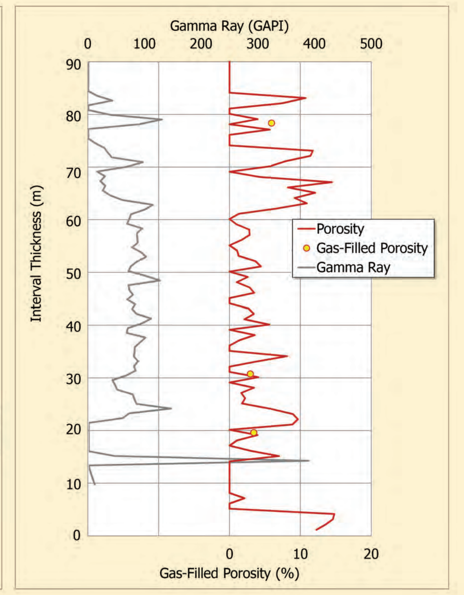

Gas-filled porosity of the Chainman Shale section is shown in the left-hand log. Inferred porosity over the hypothesized hydrocarbon-bearing zones is shown in the right-hand log. The porosity could be gas- or oil-filled.

Geochemistry

Total organic carbon and programmed pyrolysis data of Chainman Shale from the Camp Canyon section (see measured section for sample locations in meters).

Sample ID	As-Received Bulk Density (g/cc)	TOC[1] (wt.%)	S1[2] (mg/g)	S2[3] (mg/g)	S3[4] (mg/g)	Tmax[5] (°C)	HI[6]	OI[7]	S1/TOC	PI[8]	Calc R_o[9] (%)
Sample 486	2.325	0.70	0.02	0.11	0.46	NA	16	66	3	0.15	NA
Mc-8-51	NA	0.68	0.04	0.07	0.22	NA	10	32	6	0.36	NA
Mc-8-49	2.399	0.61	0.04	0.18	0.15	NA	30	25	7	0.18	NA
Mc-7-42	NA	1.27	0.04	0.28*	0.29	468	22	23	3	0.13	1.26
Mc-7-39	NA	1.57	0.19	1.08	0.28	438	69	18	12	0.15	0.72
Mc-9-86	2.504	1.26	0.08	0.74	0.38	448	59	30	6	0.10	0.90
Mc-6-16b	2.409	1.63	0.04	0.16	0.55	NA	10	34	2	0.20	NA
Mc-6-9	NA	1.17	0.03	0.23	0.35	NA	20	30	3	0.12	NA
Mc-6-6	2.633	1.58	0.32	1.59	0.17	446	101	11	20	0.17	0.87
Mc-6-2	2.593	0.94	0.20	1.02	0.36	445	108	38	21	0.16	0.85
Basal Chainman	NA	3.40	0.04	0.92	0.97	511*	27	29	1	0.04	2.04

[1]TOC = total organic carbon (wt.%)
[2]S1 = amount of free hydrocarbons in the sample (mg HC/g rock)
[3]S2 = amount of hydrocarbons generated by pyrolitic degradation of kerogen (mg HC/g rock)
[4]S3 = amount of CO_2 (mg CO_2/g rock) produced during pyrolysis of kerogen
[5]Tmax = temperature (°C) of maximum release of hydrocarbons from cracking of kerogen during pyrolysis
[6]HI = hydrogen index
[7]OI = oxygen index
[8]PI = production index
[9]R_o = calculated vitrinite reflectance
*Data questionable due to outcrop sampling conditions.

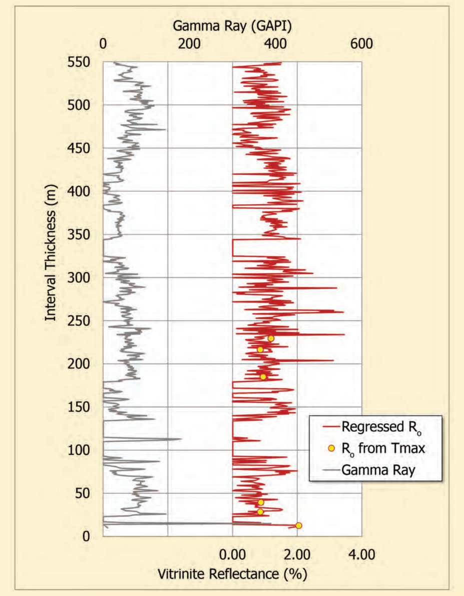

The total gamma-ray track from hand-held measurements and laboratory measured values for vitrinite reflectance (calculated from Tmax) are shown. The multivariate regressed curve was based on the discrete measurements and the spectral gamma-ray data, and should be considered as approximate.

The total gamma-ray track from hand-held measurements and the laboratory measured values for TOC are shown. The multivariate regressed curve was based on the discrete measurements and the spectral gamma-ray data, and should be considered as approximate.

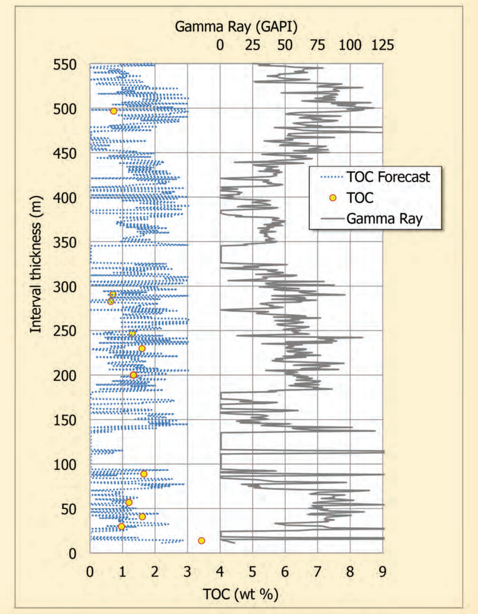

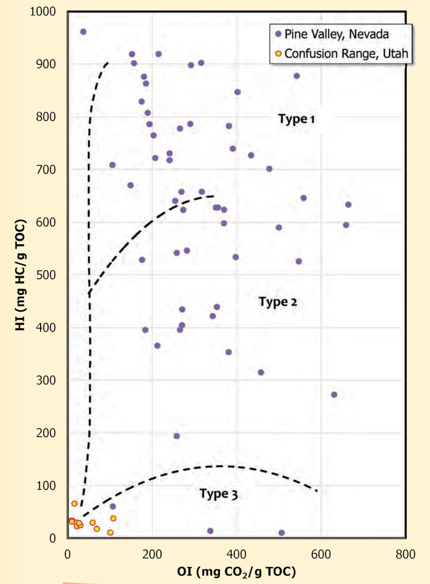

Van Krevelen diagram showing TOC measurements from the collected samples from the Confusion Range in western Utah (yellow circles) and legacy data from Aminoil No. 1-23 Land Co. well, Pine Valley, Nevada (from Poole and Claypool, 1984).

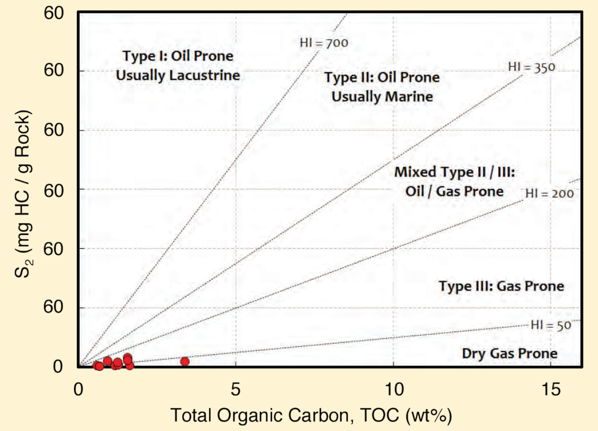

Hydrocarbon generation (S2) versus TOC suggests that the kerogen is gas to dry-gas prone.

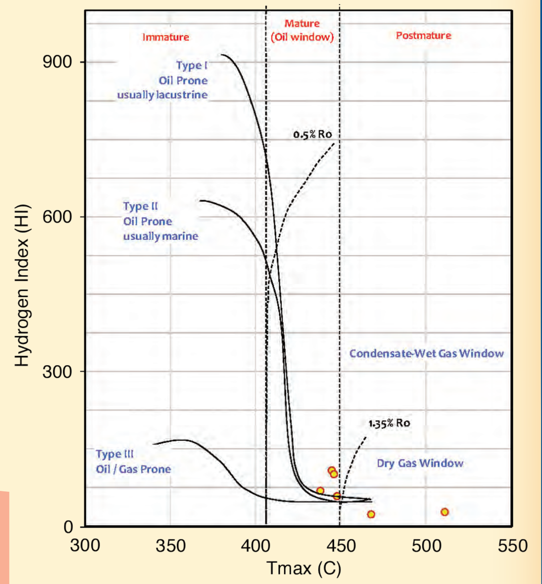

This plot of hydrogen index (HI) versus Tmax suggests the possibility of oil as well as dry gas.

Resource Calculations

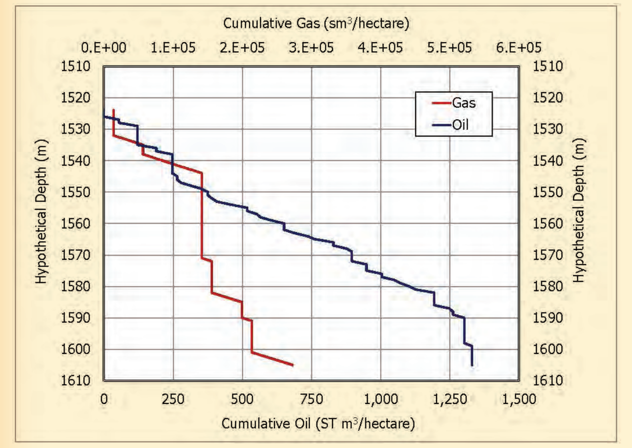

Possible cumulative volumes (recoverable estimate) of oil (blue line) and gas (red line) for a hypothetical Chainman completion. The estimates suggest that prospective oil and gas production in the Chainman Shale is a possibility. Permeabilities are low but economic recovery is feasible if the assumptions made are anywhere reasonably realistic.

What If – Hypothetical Estimates

The basis of the resource calculations incorporated the following conditions and assumptions.

1. Depth was specified as 1524 m (5000 ft) TVD. The top of the Skunk Spring Limestone Member of the Chainman Shale was set at this depth.
2. Reservoir pressure was assumed to be hydrostatic (~10.4 kpa/m, 0.45 psi/ft).
3. Reservoir pressure for oil was assumed to be above the bubble point.
4. A temperature gradient was assumed to be 2.5°C/100 m (1.38°F/100 ft) (Blackett, 2004).
5. Oil gravity was assumed to be 32°API. Gas gravity was taken as 0.65 and presumed to be methane only.
6. Separator pressure was assumed to be 1 MPa (145 psi) and Standing's (1977) relationship was used to calculate the oil formation volume factor.
7. Water saturation was assumed to be 20% on average.
8. Compressible storage only was assumed. This is conservative since some adsorption could be anticipated.
9. For gas production, methane only was assumed. In this reservoir, there is the possibility of some heavier components also being present.
10. The following criteria were required.
    a. TOC must be greater than 0.5% with finite porosity,
    b. for oil production the vitrinite reflectance must be between 0.6 and 1.1%, and
    c. for gas production the vitrinite reflectance must be greater than 1.1%.
11. Initial in-situ volumes were estimated per hectare.

Using these reservoir parameters, estimation of cumulative production of 270,000 barrels of oil (BO) and 1.5 billion cubic feet of gas (BCFG) over a 20-year lifespan might be recovered from a vertical, fully penetrating well on an 80-acre spacing.

Conclusions

- Three organic shale facies as measured in the central Confusion Range section from the Mississippian Chainman Shale exhibit hydrocarbon potential: (1) a stratigraphically pervasive calcareous mudrock, (2) a siliceous-calcareous facies, and (3) a noncalcareous argillaceous facies. These are found in the Delle Phosphatic, uppermost Needle Siltstone, and lower Camp Canyon Members.
- Nonshale facies that also possess potential include a dolomitic siltstone near the base of the formation, and the Delle Phosphatic Member (phosphorite deposits) that rest directly upon the Joana Limestone.
- Geochemical work indicates that the Chainman contains acceptable TOC values to be considered a viable hydrocarbon source, but these surface sample numbers (~1 to 2 wt.%) are modest. The Tmax values fall in the oil window and perhaps in the oil-wet gas category. Mobile oil was found in one of the collected surface samples.
- Other TOC contributors may include nonanalyzed dark, micritic limestone beds found interbedded with the mudrocks in the lower portion (Delle Phosphatic Member through lower Camp Canyon Member) of the central Confusion Range section.
- Mudrock porosities are acceptable for hydrocarbon production potential as compared to other shale-gas or shale-oil reservoirs. The siliceous-calcareous facies showed ~9.5% effective porosity, although all permeability measurements scarcely attain the 100 nD measurement, an empirically pre-determined value perhaps minimally essential for economic recoveries. Again, surface weathering effects may also have occurred here.
- A surface gamma-ray log, generated for this study, might prove an invaluable analog for any wells penetrating the Chainman in this vicinity.
- Hypothetical oil-in-place measurements and estimated hydrocarbon recoveries are also encouraging. Recoverable hydrocarbons on an 80-acre spacing is estimated at 270,000 BO and 1.5 BCFG per well.
- Economic gas recoveries were recently attained from the Chainman from a well (currently confidential) in Railroad Valley, Nevada. The well was shut-in because of lack of gas transmission facilities.

Acknowledgements

This research was funded through the Utah Geological Survey (UGS), Contract #112610, under the "Characterization of Utah's Hydrocarbon Reservoirs, Metals, and Industrial Minerals Program." Additional funding was provided by Bereskin and Associates, Inc. Craig Poole (Fresno City College), Tom Oesleby (consultant), and Dave Taff (consultant) measured sections, and collected and cataloged samples. We thank Steve Herbst and Tom Dempster of the UGS for conducting gamma-ray field measurements and assisting with field sample collection. Peter Nielsen (UGS) produced gamma-ray profiles. Geochemical analysis, SEM, and TRA were provided by TerraTek, a Schlumberger Company. Tarn Bereskin (Bereskin and Associates, Inc.) conducted geologic reconnaissance to identify a specific section of Chainman Shale suited for detailed study and produced graphs of the section. Cheryl Gustin and Jay Hill of the UGS assisted with figure preparation. The poster was designed and prepared by Stevie Emerson and Nikki Simon of UGS.

References

Blackett, R.E., 2004, Geothermal gradient data for Utah: Geothermal Resources Council Transactions, v. 20, p. 3–6.

Hintze, L.F., Davis, F.D., 2003, Geology of Millard County, Utah: Utah Geological Survey Bulletin 133, 305 p.

Poole, F.G., and Claypool, G.E., 1984, Petroleum source-rock potential and crude-oil correlation in the Great Basin, in Woodward, J., Meissner, F.F., and Clayton, J.L., editors, Hydrocarbon source rocks of the greater Rocky Mountain region: Denver, Rocky Mountain Association of Geologists Guidebook, p. 179-229.

Sadlick, Walter, 1965, Biostratigraphy of the Chainman Formation, eastern Nevada and western Utah: Salt Lake City, University of Utah, Ph.D. dissertation, 227 p.

Sandberg, C.A., Poole, F.G., and Gutschick, R.C., 1980, Devonian and Mississippian stratigraphy and conodont zonation of Pilot and Chainman Shales, Confusion Range, Utah, in Fouch, T.D., and Magathan, E.R., editors, Paleozoic paleogeography of the west-central United States: Denver, Rocky Mountain Section, Society of Economic Paleontologists and Mineralogists, p. 71-79.

Standing, M.B., 1977, Volumetric and phase behavior of oil field hydrocarbon systems: Dallas, Texas, Society of Petroleum Engineers, 150 p.

Disclaimer